Development 138, 3545-3555 (2011) doi:10.1242/dev.068148

Notch and Ras promote sequential steps of excretory tube development in *C. elegans*

Ishmail Abdus-Saboor[1,*], Vincent P. Mancuso[1,*], John I. Murray[1], Katherine Palozola[1], Carolyn Norris[2], David H. Hall[3], Kelly Howell[1], Kai Huang[1] and Meera V. Sundaram[1,†]

SUMMARY

Receptor tyrosine kinases and Notch are crucial for tube formation and branching morphogenesis in many systems, but the specific cellular processes that require signaling are poorly understood. Here we describe sequential roles for Notch and Epidermal growth factor (EGF)-Ras-ERK signaling in the development of epithelial tube cells in the *C. elegans* excretory (renal-like) organ. This simple organ consists of three tandemly connected unicellular tubes: the excretory canal cell, duct and G1 pore. *lin-12* and *glp-1/Notch* are required to generate the canal cell, which is a source of LIN-3/EGF ligand and physically attaches to the duct during de novo epithelialization and tubulogenesis. Canal cell asymmetry and *let-60/Ras* signaling influence which of two equivalent precursors will attach to the canal cell. Ras then specifies duct identity, inducing auto-fusion and a permanent epithelial character; the remaining precursor becomes the G1 pore, which eventually loses epithelial character and withdraws from the organ to become a neuroblast. Ras continues to promote subsequent aspects of duct morphogenesis and differentiation, and acts primarily through Raf-ERK and the transcriptional effectors LIN-1/Ets and EOR-1. These results reveal multiple genetically separable roles for Ras signaling in tube development, as well as similarities to Ras-mediated control of branching morphogenesis in more complex organs, including the mammalian kidney. The relative simplicity of the excretory system makes it an attractive model for addressing basic questions about how cells gain or lose epithelial character and organize into tubular networks.

KEY WORDS: *C. elegans*, Ras, Tubulogenesis

INTRODUCTION

Many organs, such as the mammalian kidney and the vasculature, consist of complex networks of tubules that develop from clusters of initially unpolarized mesenchymal cells (Hogan and Kolodziej, 2002; Lubarsky and Krasnow, 2003; Dressler, 2009). The processes by which these cells polarize, form epithelial or endothelial junctions, and then organize into complex tubular shapes are only beginning to be elucidated. In many cases, signaling pathways involving Receptor tyrosine kinases (RTKs) and Ras are crucial for formation and patterning of the tubular network. For example, during branching morphogenesis of the ureteric bud in the kidney, signaling by the Ret RTK promotes tip cell identity and specifies the location of new branches (Shakya et al., 2005; Chi et al., 2009). Similarly, during sprouting angiogenesis, signaling by vascular endothelial growth factor receptors promotes tip cell identity (Gerhardt, 2008). Absence of RTK signaling results in renal or vascular agenesis. Although the importance of RTK pathways in controlling tube development is clear, the specific cellular behaviors that require signaling, and the downstream mechanisms that control them, are not well understood.

Tubulogenesis can be reversible, as cells can withdraw from an existing tube and give rise to different cell types. For example, venous endothelial cells in the mouse de-differentiate and divide to give rise to new coronary arteries, capillaries and veins as part of their normal developmental program (Red-Horse et al., 2010). Epithelial-to-mesenchymal transition (EMT) or endothelial-to-mesenchymal transition (EndMT) are central features of injury-induced fibrosis in the kidney and heart (Kalluri and Neilson, 2003; Zeisberg et al., 2007) and underlie the metastatic properties of many tumor cells (Kalluri and Weinberg, 2009). Tubes that form by de novo polarization may be particularly prone to EMT, but the mechanisms that promote or restrain such behaviors remain poorly understood.

The *Caenorhabditis elegans* excretory system is a simple example of an epithelial tube network. The excretory system is the worm's renal-like system and is required for fluid waste expulsion (Nelson et al., 1983; Nelson and Riddle, 1984; Buechner, 2002). It consists of three tandemly arranged unicellular tubes: the large canal cell (which runs the length of the body and appears to collect waste fluid), and the smaller duct and pore cells (which connect the canal cell to the outside environment) (Fig. 1). Whereas the canal cell and duct tubes are permanent throughout the life of the animal, the G1 pore eventually withdraws from the excretory system to become a neuroblast, at which time a neighboring epidermal cell (G2) replaces G1 as the excretory pore tube (Sulston et al., 1983; Stone et al., 2009). Thus the excretory system provides a simple, genetically tractable system for studying the dynamic control of epithelial junctions, cell shape and cell identity.

The progenitors of the excretory duct and G1 pore tubes are left/right lineal homologs that appear to compete for the duct fate (Sulston et al., 1983). In wild-type animals, the left cell always becomes the duct and adopts the position most proximal to the canal cell, whereas the right cell always becomes G1 and adopts a more distal position. However, ablation of the mother of the presumptive duct causes the presumptive G1 to adopt a duct-like

[1]Department of Genetics, University of Pennsylvania School of Medicine, Philadelphia, PA 19104, USA. [2]Department of Biology, Johns Hopkins University, Baltimore, MD 21218, USA. [3]Department of Neuroscience, Center for C. elegans Anatomy, Albert Einstein College of Medicine, Bronx, NY 10461, USA.

*These authors contributed equally to this work
[†]Author for correspondence (sundaram@mail.med.upenn.edu)

Accepted 1 June 2011

position and morphology, showing that both cells have the capacity to become a duct and suggesting some lateral inhibitory mechanism that prevents both from doing so. Both *let-60*/Ras and *lin-12 glp-1*/Notch mutants lack an excretory duct, implicating Ras and Notch in the duct versus G1 pore fate decision or some other aspect of duct development (Lambie and Kimble, 1991; Yochem et al., 1997).

Here we show that Notch and Epidermal growth factor (EGF)-Ras-ERK act sequentially during excretory tube development. We identify multiple, genetically separable requirements for signaling in controlling tube cell position, identity, shape and function. Finally, we establish the excretory duct and G1 pore system as a model for investigating many basic cell biological processes associated with tube development and EMT-coupled cell fate plasticity.

MATERIALS AND METHODS

Strains and alleles

N2 var. Bristol was the wild-type strain. Unless otherwise indicated, all strains were grown at 20°C under standard conditions (Brenner, 1974) and all mutant alleles are described in Riddle et al. (Riddle et al., 1997). *I: lag-1*(*q385*), *lag-2*(*q411*), *lag-2*(*q420*). *II: let-23*(*sy97*). *III: lin-12*(*n137*), *lin-12*(*n137n720*), *lin-12*(*n941*), *glp-1*(*q46*), *glp-1*(*q231*). *IV: eor-1*(*cs28*) (Rocheleau et al., 2002), *let-60*(*sy101sy127*), *let-60*(*n1046*), *let-60*(*n2021*), *lin-1*(*e1275*), *lin-1*(*n304*) (Beitel et al., 1995), *lin-1*(*n1761*) (Jacobs et al., 1998), *lin-3*(*n1059*), *lin-45*(*n2018*). *V: sos-1*(*cs41*) (Rocheleau et al., 2002). *X: lin-15*(*n765*), *sem-5*(*n2019*). Transgenes used are: *arIs12* (*lin-12 intra*) (Struhl et al., 1993), *arIs41* (LIN-12::GFP) (Levitan and Greenwald, 1998), *gaIs27* (LET-23::GFP) (Simske et al., 1996), *jcIs1* (AJM-1::GFP) (Koppen et al., 2001), *saIs14* (*lin-48p*::GFP) (Johnson et al., 2001), *syIs107* (*lin-3p*::GFP) (Hwang and Sternberg, 2004), *wIs78* (AJM-1::GFP) (Koh and Rothman, 2001), *xnIs17* (DLG-1::GFP) (Totong et al., 2007), *vha-1p*::GFP (Oka et al., 1997), *zuIs143* (*ref-1p*::GFP) (Neves and Priess, 2005). *qnEx59* (*dct-5p*::mcherry) was provided by Julia and David Raizen (University of Pennsylvania, Philadelphia, PA, USA) and contains 845 bp of the *dct-5* 5′ region. *csIs55* (GFP::MLS-2) was generated from a pYJ59-containing array (Jiang et al., 2005) by gamma-irradiation-induced integration. *csEx146* (*lin-48p*::mcherry) contains 4.8 kb of the *lin-48* 5′ region and mcherry in vector pPD49.26 (Fire et al., 1990). *lin-3* overexpression was achieved with an integrated *lin-3p*::LIN-3::GFP transgene provided by Min Han.

Marker analysis and imaging

Images were captured by differential interference contrast (DIC) and epi-fluorescence microscopy using a Zeiss Axioskop and Hamamatsu C5985 camera, or by confocal microscopy using a Leica SP5. Images were processed for brightness and contrast using Photoshop or ImageJ. Some AJM-1::GFP images were inverted for clarity.

For electron microscopy, embryos were mounted on an agarose pad and observed under light microscopy to identify time points for fixation. A laser was used to place three to four holes in the eggshell, allowing the embryo to be aldehyde fixed while on the pad (see more details at www.wormatlas.org/laserhole.htm). The fixed embryo was postfixed with osmium tetroxide, potassium ferrocyanide and tannic acid, and then post-stained with uranyl acetate before embedding in plastic resin. Transverse serial thin sections were collected on slot grids and photographed on a Philips CM10 electron microscope. The G1 and duct cells were identified within a series of 600 serial thin sections on the basis of their positions relative to the canal cell and to the G2 and W epidermal cells (see Fig. S1 in the supplementary material) and by comparison with known nuclear positions in time-lapse confocal movies.

To visualize the duct and pore progenitor migration paths and timing, we generated 3D confocal movies of strains UP2051 (pie-1::mCherry::HIS-58::pie-1utr; his-72pro::HIS-24::mCherry::let-858utr; GFP::MLS-2) and RW10890 (pie-1::mCherry::HIS-58::pie-1utr; his-72pro::HIS-24::mCherry::let-858utr; PAL-1::GFP) as previously described (Murray et al., 2006) on a Leica TCS SP5 resonance-scanning confocal microscope with 0.5 μm *z*-slice spacing and 1.5 minute time point spacing. Temperature was 22.5°C. We used a hybrid blob-slice model and StarryNite (Bao et al., 2006; Santella et al., 2010) for automated lineage tracing and curated the duct, pore and canal lineages (ABplpaa and ABprpaa) through ventral enclosure (approximately 275 minutes) with AceTree (Boyle et al., 2006).

Ablations

Laser ablations were performed with a Micropoint Laser Ablation system (Photonic Instruments, St Charles, IL) mounted to a Leica DM5500B or Zeiss Axiophot microscope. The canal cell mother (ABplpappaa) was identified using *zuIs143* (*ref-1p*::GFP) (Neves and Priess, 2005). Successful ablation was confirmed by the absence of the canal cell as assessed by DIC and either *vha-1p*::GFP or AJM-1::GFP patterns.

Immunostaining

Embryos were permeabilized by freeze-cracking and fixed in methanol as described (Duerr et al., 1999) and incubated with primary antibodies overnight at 4°C and with secondary antibodies for 2 hours at room temperature. The following antibodies were used: preadsorbed rat anti-MLS-2 (CUMCR6; 1:400) (Jiang et al., 2005) goat polyclonal anti-GFP (Rockland; 1:50), rabbit polyclonal anti-DLG-1 (1:50 to 1:100) (Segbert et al., 2004). All secondary antibodies were from Jackson ImmunoResearch Laboratories and were used at a dilution of 1:50 to 1:200.

RESULTS

Excretory tube development involves de novo formation and remodeling of epithelial junctions

Excretory tube development occurs in three broad phases (migration/tubulogenesis, morphogenesis/differentiation and G1 withdrawal/remodeling) (Fig. 1A) (Sulston et al., 1983; Buechner, 2002; Berry et al., 2003; Stone et al., 2009). To visualize the excretory duct and G1 pore during these phases, we used lineage-specific markers in combination with epithelial apical junction markers AJM-1 (Koppen et al., 2001) and DLG-1/Discs Large (Bossinger et al., 2001) (Fig. 1). GFP::MLS-2 marked all ABpl/rpaaa descendants (including the duct and G1) plus additional lineages during ventral enclosure (Yoshimura et al., 2008) (J.I.M., unpublished) (Fig. 1B-C,E), whereas *dct-5p*::mCherry marked the duct, G1 and some other epithelial cells during L1 (this work, Fig. 1J-K). We also analyzed a ventral enclosure embryo by transmission electron microscopy (TEM) of serial sections (Fig. 1D; see Fig. S1 in the supplementary material) and traced the canal, duct and G1 pore lineages through ventral enclosure from 3D confocal movies of eight histone::mCherry-expressing embryos (Materials and methods).

The canal cell, duct and G1 pore progenitors are born in disparate locations of the embryo. During ventral enclosure (Fig. 1B-E), the duct (left) and G1 pore (right) progenitors migrated toward the canal cell, which is located slightly left of the ventral midline. The duct progenitor had a shorter distance to migrate, and it appeared to reach the canal cell first (Fig. 1C). TEM of an embryo at ventral enclosure showed the duct progenitor and the canal cell closely apposed, whereas the G1 progenitor was excluded from the canal cell by the duct and other intervening cell bodies (Fig. 1D). In 6/8 3D confocal movies, the duct nucleus arrived adjacent to the canal cell about 5-10 minutes before G1. At this time, one to two nuclei still separated the canal from G1; the most consistent of these was RIS, a right-derived neuron with a left homolog that is related to the canal cell and that undergoes programmed cell death. In 2/8 movies, the duct and G1 nuclei arrived near the canal cell at approximately the same time, so it was not possible to determine which cell contacted the canal cell first in the absence of a

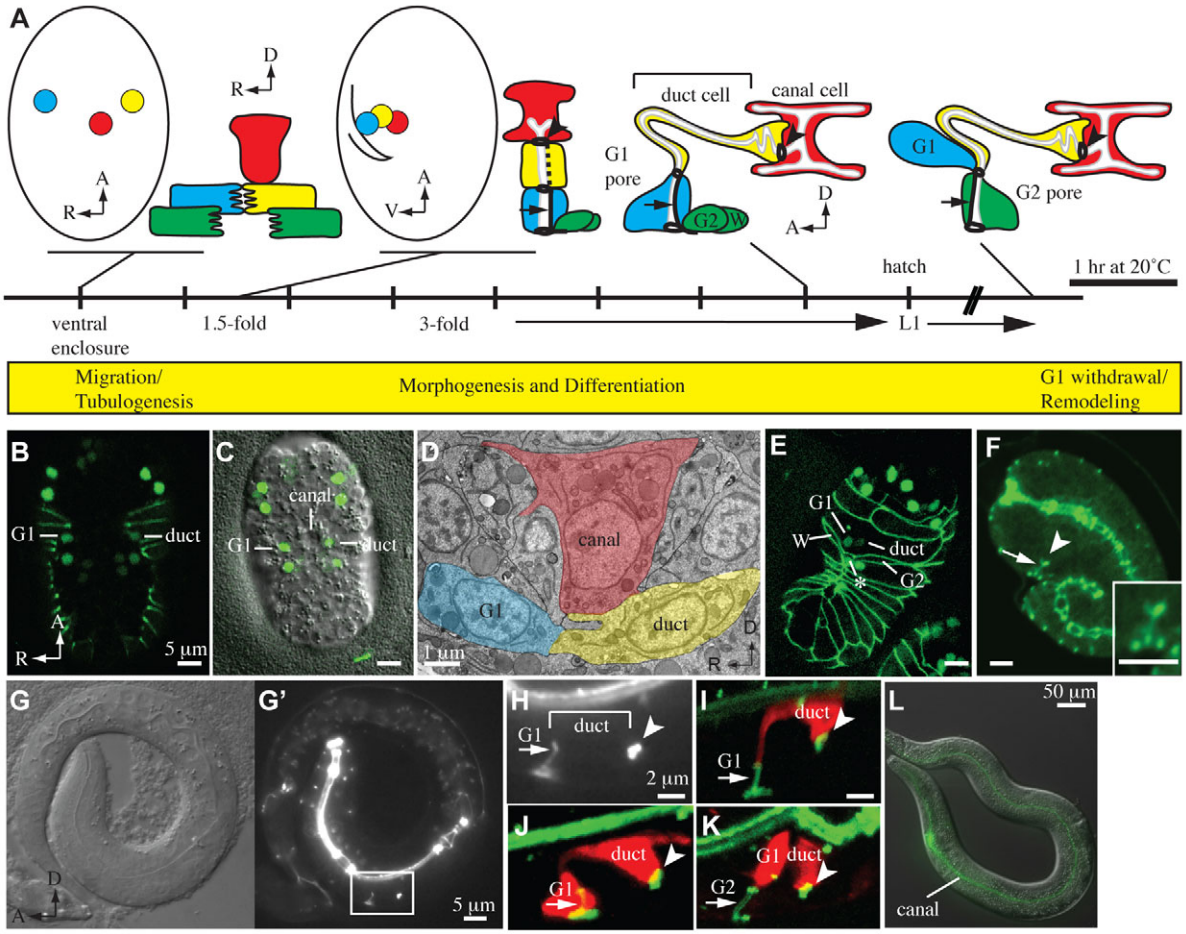

Fig. 1. Timeline of excretory system development. (**A**) Schematics of excretory canal cell (red, ABplpappaap), duct (yellow, ABplpaaaapa), G1 (blue, ABprpaaaapa), G2 (green, ABplapaapa) and W (green, ABprapaapa) at different developmental stages, based on Sulston et al. (Sulston et al., 1983), prior electron microscopy (Stone et al., 2009) and this work. Dark black lines, apical junctions; dotted line, duct auto-fusion; arrow, pore autocellular junction; arrowhead, duct-canal cell intercellular junction; bracket, duct cell body. Not shown are the non-essential excretory gland cells, which also connect to the duct-canal junction (Nelson et al., 1983; Nelson and Riddle, 1984). (B-E) Progressively older ventral enclosure stage embryos. (B-C,E) Ventral views. GFP::MLS-2 marks the presumptive duct and G1 pore nuclei. DLG-1::GFP marks epidermal cell junctions in B and E, which are confocal projections. (**B**) The presumptive duct and G1 initially lack junctions. (**C**) The presumptive duct is closer to the canal cell than is the presumptive G1. (**D**) TEM of a wild-type embryo at a similar stage to C, with cells pseudo-colored as in A. Transverse anterior view. The presumptive duct and G1 have met at the ventral midline. The duct makes extensive contact with the canal cell, while G1 is excluded. No epithelial junctions or lumen are detectable. (**E**) G1 moves ventrally. The asterisk indicates the site of future G1 pore opening between G2 and W epidermal cells (see also Fig. S1 in the supplementary material). (F-L) Left lateral views. (**F**) 1.5-fold stage embryo immunostained for DLG-1, showing newly formed autocellular junctions (inset) just before duct auto-fusion. (**G-K**) L1 larvae. The box in G′ indicates the region magnified in H. AJM-1::GFP marks junctions. The duct no longer has an autocellular junction. (I) *lin-48p*::mcherry marks the duct. (J) *dct-5p*::mcherry marks the duct and G1 pore in early L1 and (K) the duct and G1 in late L1 after G1 withdrawal and G2 entry. (**L**) Adult canal cell marked with *vha-1p*::GFP. Note that the canal cell elongates extensively.

membrane or cytoplasmic label. After the duct reached the canal cell, they began to ingress, while G1 moved to a ventral position between the G2 and W epidermal cells (Fig. 1E). Together, these observations suggest that asymmetry of the canal cell and its lineal relatives might contribute to asymmetry in duct and G1 pore behavior.

The cells initially lacked epithelial junctions (Fig. 1B,D), but after they contacted each other, they formed epithelial junctions and underwent tubulogenesis (Fig. 1F). As described previously (Stone et al., 2009), the duct and G1 pore cells wrapped up into tube shapes and formed autocellular junctions. G1 retained this autocellular junction, but the duct cell rapidly auto-fused, becoming a seamless toroid. The canal cell formed lumen intracellularly at the site of the duct-canal cell intercellular junction. By the 1.5-fold stage, the canal cell, duct and pore formed a simple block-like stack of tandemly connected unicellular tubes with a continuous lumen and prominent epithelial junctions (Fig. 1A,F).

Further morphogenesis occurred during the latter part of embryogenesis, such that by the first larval stage, the excretory duct (Fig. 1G-J) and canal cell (Fig. 1L) had distinctive elongated shapes. The cells also began expressing unique differentiation markers, such as the *lin-48*/Ovo transcription factor in the duct (Fig. 1I) (Johnson et al., 2001).

G1 withdrawal and G2 entry occurred in the first larval stage, after the excretory system had already begun to function. At this time, G1 migrated dorsally and lost its epithelial junctions while a neighboring epidermal cell, G2, formed an autocellular junction and replaced it as the pore (Fig. 1K) (Sulston et al., 1983; Stone et

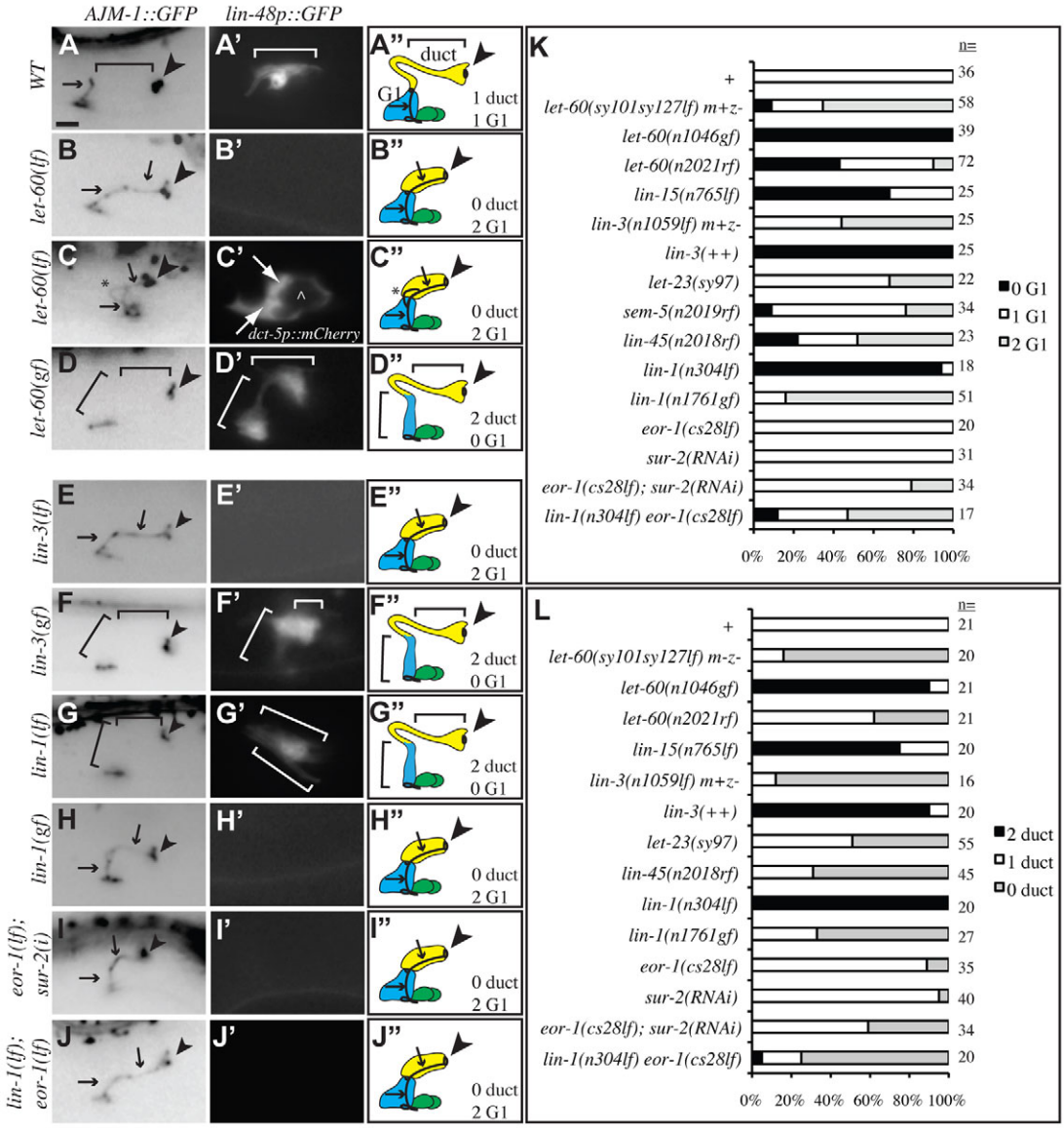

Fig. 2. *let-60/Ras* promotes the duct versus G1 pore fate. (**A-J′**) AJM-1::GFP (left column) and *lin-48p*::GFP or (C′) *dct-5p*::mCherry (middle column) expression in L1 larvae of the indicated genotypes. Lateral views, with schematic interpretations (right column) and symbols as in Fig. 1. Colors represent lineal identity, not fate. Mutants with reduced signaling usually have two pore-like cells with autocellular junctions, but as fluid (carat) accumulates during L1 (C), large junctional rings (asterisk) are common. In (C′), white arrows indicate two stacked pore-like cells. Mutants with increased signaling have a seamless binucleate duct that connects to the ventral epidermis. (**K**,**L**) Quantification of marker phenotypes. Note that some mutants with '0 G1' have defects in cell stacking and tubulogenesis rather than in cell fate specification (see Fig. 4). Scale bar: 2 μm.

al., 2009). G2 subsequently divides in L2 to generate a neuronal daughter (G2.a) and an epithelial daughter (G2.p) that replaces it as the permanent pore tube (Sulston and Horvitz, 1977). Throughout this time the duct process must remodel its ventral junction to connect to its new partners.

let-60/Ras is both necessary and sufficient for duct versus G1 pore fate specification

let-60/Ras is required cell autonomously within the excretory duct cell for proper excretory system function and organismal viability and was previously proposed to promote the duct versus G1 pore fate (Yochem et al., 1997). To test this model, we used AJM-1::GFP and *lin-48p*::GFP markers to examine *let-60 ras* mutants (Fig. 2).

Most *let-60*(*sy101sy127lf*) null mutants, obtained from heterozygous mothers, had two pore-shaped cells with autocellular junctions and no *lin-48p*::GFP (Fig. 2B-C,K-L), consistent with a duct-to-G1 pore cell fate transformation. Although the mutants lacked a duct-like cell, the overall arrangement of the excretory system resembled that of wild-type animals: two cells were arranged in tandem, with one contacting the canal cell and the other contacting the ventral epidermis. Thus, initial migration, stacking and tubulogenesis appeared normal, but auto-fusion did not occur and duct-specific differentiation markers were not expressed.

let-60(*sy101sy127lf*) mutants died as late L1 larvae with a rigid, fluid-filled appearance termed 'rod-like lethality'. Fluid first accumulated near or within the two pore-like tubes (Fig. 2C′).

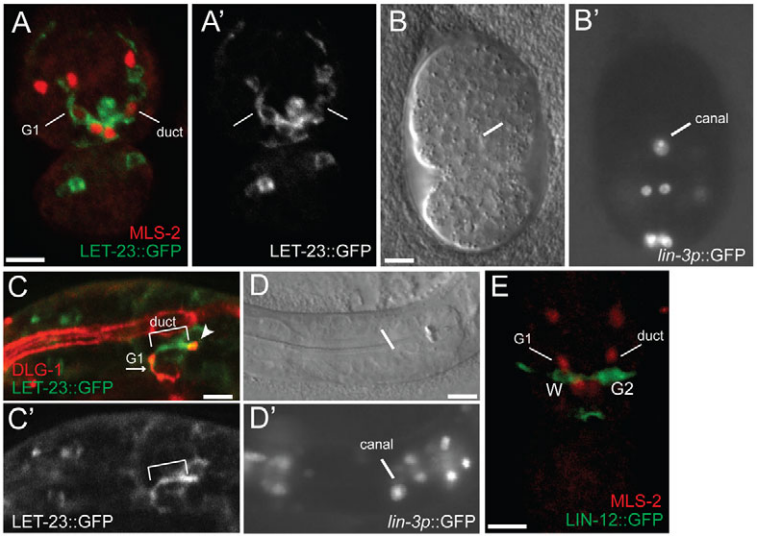

Fig. 3. *lin-3*/EGF, *let-23*/EGFR and *lin-12*/Notch reporter expression in the excretory system. (**A**,**C**) LET-23::GFP is expressed in the presumptive duct and G1 pore at ventral enclosure (A) and in the duct (bracket) at 3-fold (C). (**B**,**D**) *lin-3p*::GFP is expressed in the canal cell from ventral enclosure (B) through L1 (D). (**E**) LIN-12::GFP is expressed in the presumptive G2 and W but not in the presumptive duct or pore at ventral enclosure. In A, C and E, embryos were co-stained with anti-GFP and either anti-MLS-2 or anti-DLG-1 to mark the duct and G1 pore (n>10 each). Scale bars: 5 μm.

Notably, the timing of fluid accumulation in mid-L1 coincided with the normal timing of pore remodeling and is often associated with large junctional rings or discontinuities (Fig. 2C). As withdrawal from the excretory system is a normal feature of G1 pore identity, withdrawal of both pore-like cells may explain the inviability.

let-60(*n1046gf*) hypermorphic mutants had two duct-like nuclei expressing *lin-48p*::GFP and no autocellular junctions (Fig. 2D,K-L), consistent with a G1 pore-to-duct cell fate transformation. The two duct cells fused to form a binucleate cell, as would be predicted for two adjacent cells expressing the fusogen *aff-1*, which is required for duct auto-fusion (Stone et al., 2009) and generally sufficient for fusion of adjacent cells (Sapir et al., 2007). Removal of *aff-1* in a *let-60*(*gf*) background restored both intercellular and autocellular junctions (data not shown). The binucleate duct cell attached to the ventral epidermis, allowing for fluid excretion, and was permanent throughout the life of the animal.

We conclude that Ras signaling is both necessary and sufficient to promote duct versus G1 pore identity, and that identity can be uncoupled from cell position. Notably, however, some *let-60* null mutants still possessed a cell with at least partial duct-like character (Fig. 2K-L). Evidence below suggests that this is a result of maternally provided *let-60* activity; maternal activity could not be completely removed in our experiments because of the requirements for *let-60* and other pathway components in germline development (Church et al., 1995).

let-60/Ras functions within the canonical EGF-Ras-ERK pathway to promote the duct fate

Animals mutant for *lin-3*/EGF or various other components of the canonical EGF-Ras-ERK pathway all display a rod-like lethal phenotype associated with excretory system failure (Ferguson and Horvitz, 1985; Sundaram, 2006). We examined mutants for *lin-3/EGF* and *lin-1/Ets*, which lie at the beginning and end of this pathway, respectively (Hill and Sternberg, 1992; Beitel et al., 1995). *lin-3*(*lf*) and *lin-1*(*gf*) mutants appeared similar to *let-60*(*lf*) mutants, and *lin-3* overexpression and *lin-1*(*lf*) mutants appeared to be similar to *let-60*(*gf*) mutants (Fig. 2E-H,K-L). Furthermore, a variety of other Ras pathway mutants examined (including hypomorphic alleles of *let-23/EGFR* and *lin-45/Raf*) also showed evidence of duct-to-pore fate transformations (Fig. 2K-L). Finally, *eor-1* and *sur-2* are nuclear factors that act redundantly downstream of MPK-1/ERK (Singh and Han, 1995; Tuck and Greenwald, 1995; Howard and Sundaram, 2002); *eor-1* also appears to act redundantly with a cryptic positive function of *lin-1*/Ets (Howard and Sundaram, 2002; Tiensuu et al., 2005). We found that *eor-1; sur-2*(*RNAi*) and *lin-1 eor-1* double mutants frequently had two pore-like cells (Fig. 2I-L). These data are consistent with the entire canonical pathway promoting duct versus G1 pore identity.

During this analysis, we noted that some mutants with reduced signaling had paradoxical ‘0 G1’-like junction patterns, without concomitant duct fate duplication, or had excretory failure despite apparently normal junction patterns and fates (Fig. 2K-L). These observations suggested that Ras signaling plays roles beyond cell fate specification (see below).

The excretory canal cell expresses *lin-3*/EGF

As the mutant analyses above suggest that signaling by LIN-3/EGF through LET-23/EGFR is responsible for LET-60/Ras activation in the duct, we asked where these proteins are expressed. Consistent with the fact that both cells can respond to LIN-3 to adopt the duct fate, a functional LET-23::GFP reporter, *gaIs27* (Simske et al., 1996), was expressed in both presumptive duct and G1 pore cells during ventral enclosure (Fig. 3A). To examine *lin-3* expression, we used a *lin-3* promoter::GFP reporter (*syIs107*) that contains ~2.5 kb of upstream regulatory sequence as well as the first *lin-3* intron (Hwang and Sternberg, 2004). Most notably, *lin-3p*::GFP was strongly expressed in the excretory canal cell, beginning soon after canal cell birth and continuing into early larval development (Fig. 3B,D). *lin-3p*::GFP was also expressed in a variety of other cells further away from the presumptive duct and G1 pore. These data suggested that the canal cell might be a relevant source of the duct-inducing signal, a model that fits with the observation that the left member of the equivalence group, which is closest to the canal cell, is the cell that normally adopts the duct fate.

Ras signaling promotes cell stacking and a canal-cell-proximal position

EGF-Ras signaling could promote duct versus G1 pore cell fate specification independently of cell stacking and tubulogenesis, or signaling could also control initial cell positioning. The latter possibility was suggested by results of a prior mosaic analysis, in which a *let-60*(+) presumptive G1 cell could outcompete a *let-60*(–) presumptive duct cell for the more dorsal, canal-cell-proximal position and take on the duct fate (Yochem et al., 1997).

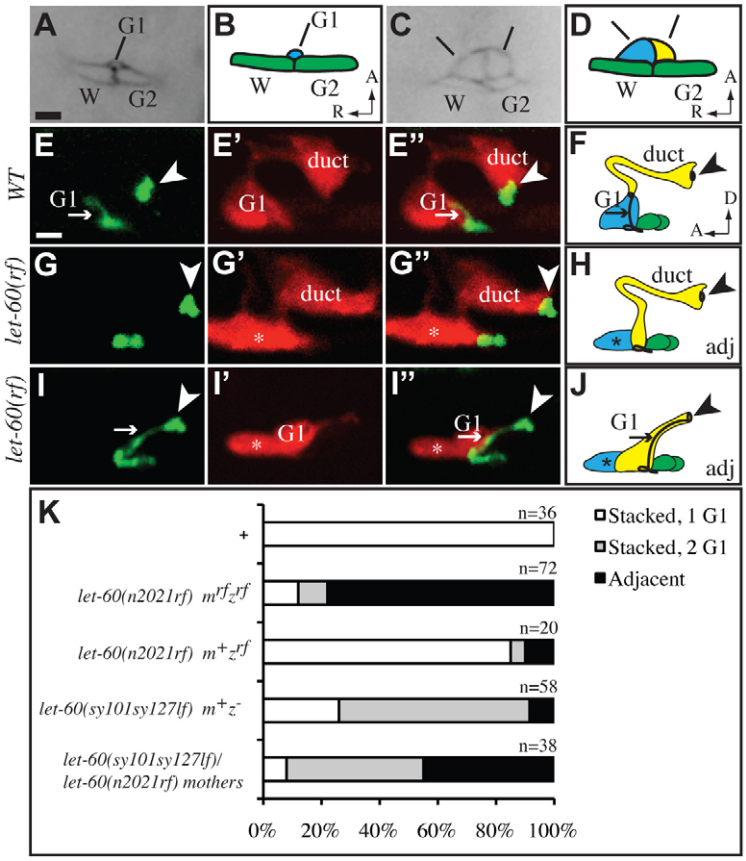

Fig. 4. *let-60/Ras* hypomorphs reveal defects in cell competition and stacking. (**A**,**B**,**E**,**F**) Wild-type. (**C**,**D**,**G-J**) *let-60*(*n2021rf*). (A,C) AJM-1::GFP in threefold embryos, ventral view. Lines indicate ventral junctions between the presumptive G1 or duct and the epidermis. (E,G,I,K) AJM-1::GFP and *dct-5p*::mCherry in early L1s, lateral view. Asterisks indicate ventral cells with neither duct-like nor pore-like morphology. In *let-60*(*n2021rf*) mutants, the presumptive duct and G1 adopt adjacent positions in the epidermis (C,D) and one cell usually reaches from the ventral epidermis to the canal cell (G-J). The lineal identity of this cell is unknown and may be variable. (**K**) Quantification of adjacent defects in early L1 larvae from heterozygous versus homozygous mutant mothers. Animals with no G1 pore autocellular junction or with a single autocellular junction that stretched from the ventral epidermis to the canal junction were scored as 'adjacent'.

Consistent with a model in which both cells compete for the canal-cell-proximal position, animals homozygous for a partial loss-of-function allele, *let-60*(*n2021*), displayed a variable phenotype in which the presumptive duct and G1 cells often adopted adjacent positions rather than stacking on top of each other (Fig. 4C-D). In many of these cases, a single duct-like cell reached from the ventral epidermis to the canal cell, while the second cell was mispositioned to the side and appeared to be non-tubular, giving a '1 duct, 0 G1' phenotype (Fig. 4G-H). In other cases, a single pore-like (un-induced) cell reached from the ventral epidermis to the canal cell, giving a '0 duct, 1 G1' phenotype (Fig. 4I-J). Similar defects were seen in other hypomorphic mutants and in *lin-1; eor-1* double mutants (Fig. 2K and data not shown). We conclude that Ras signaling influences duct and G1 pore stacking.

Notably, the adjacent phenotype was observed only occasionally in *let-60* or *lin-3* null mutants obtained from heterozygous mothers (Fig. 2K, Fig. 4K). This is in part because of maternal rescue, as most *let-60*(*n2021rf*) mutants obtained from heterozygous mothers also had normal cell stacking, in contrast to those obtained from homozygous mutant mothers (Fig. 4K). Nevertheless, progeny from *let-60*(*sy101sy127lf*)/*let-60*(*n2021rf*) mothers had a lower frequency of adjacent cells than those from *let-60*(*n2021rf*) mothers (Fig. 4K). Therefore, the adjacent phenotype may reflect problems in resolving cell competition under circumstances in which Ras signaling is sub-optimal but not absent (see Discussion).

The canal cell is required for stacking and tubulogenesis of the duct and G1 pore

To test if LIN-3/EGF expression by the canal cell is required for duct fate specification or cell stacking, we first removed the canal cell (or its mother) physically by laser ablation. In the absence of the canal cell, most animals still had a *lin-48p::GFP*+ cell (Table 1), indicating that other sources of LIN-3 are sufficient to induce at least some features of duct identity. However, duct morphology was abnormal and the G1 pore autocellular junction was missing (Fig. 5L-M), suggesting that stacking had been disrupted.

We next examined the effects of removing the canal cell genetically using Notch mutants. Mutants lacking both *C. elegans* Notch receptors, LIN-12 and GLP-1, the DSL ligand LAG-2 or the CSL transcription factor LAG-1 have a constellation of defects referred to as the 'Lag' (*lin-12* and *glp-1*) phenotype (Lambie and

Table 1. Physical or genetic removal of the canal cell reduces but does not prevent duct fate specification

	Percentage of animals			
Genotype†	Canal cell	*n*	Duct cell	*n*
+	100	32	97	31
+, canal cell ablated	0	9	100	9
+, canal cell parent ablated	0	8	87	8
lin-12(*n941lf*) *glp-1*(*q46lf*) *m+z–*	0	30	47	30
lag-1(*q385lf*) *m+z–*	0	32	95	40
lag-2(*q411lf*) *m+z–*	3	34	44	25
lag-2(*q420rf*)	+	31	94	31
lag-2(*q420rf*)	–	34	38	34
lin-12(*n137gf*)	+	15	100	69
arIs12 [lin-12(intra)]	+	40	97	40

*Presence of the canal cell or duct cell was assessed based on *vha-1p*::GFP or *lin-48p*::GFP reporter expression, respectively. + or – indicate that presence of canal cell was assessed based on nuclear morphology or AJM-1::GFP.
†*m+z–* indicates that larvae were obtained from heterozygous *hT2[qIs48]* balancer mothers. For canal cell parent ablation, strain contained *ref-1p*::GFP to aid in target identification.
lf, loss-of-function; rf, reduced function; gf, gain-of-function.

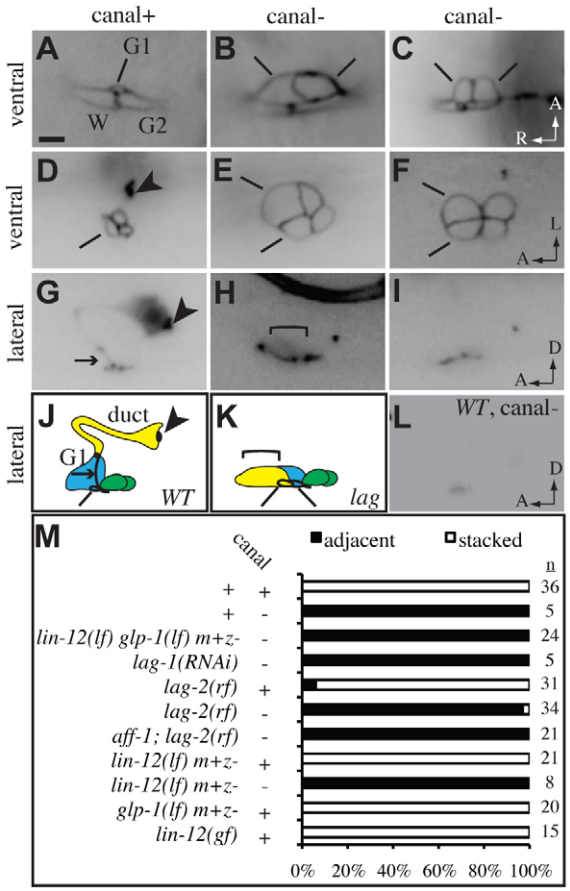

Fig. 5. The canal cell is required for duct and G1 pore stacking and tubulogenesis. (A-I,L) AJM-1::GFP. D,G,H also contain *lin-48p*::GFP. (J,K) Schematic diagrams. (**A-C**) Early threefold embryos, ventral view. (**D-F**) Early L1s, ventral view. (**G-L**) Early L1s, lateral view. In wild-type (A), the G1 pore contacts G2 and W in the ventral epidermis. In *lag-1*(*RNAi*) (B) or *lin-12*(*n941*) *glp-1*(*q46*) double mutants (C,F,I), the presumptive duct and G1 pore (lines) both contact the epidermis and lack autocellular junctions. In *lag-2*(*q420rf*) mutants (D,E,G,H), the presence of a canal cell (D,G) correlates with normal duct and G1 pore morphology. *aff-1*(*tm2214*) (E) has no impact on the *lag-2*(*q420rf*) phenotype. (L) Ablation of the canal cell mother eliminates the G1 pore autocellular junction. (**M**) Quantification of junction phenotypes in early L1 larvae. Animals with no G1 pore autocellular junction were scored as 'adjacent'. Scale bar: 2 μm.

Kimble, 1991). *lag* mutants lack an excretory canal cell owing to a lineage transformation affecting the canal cell's great-grandmother ABplpapp (Lambie and Kimble, 1991; Moskowitz and Rothman, 1996). As in canal-cell-ablated animals, *lag* mutants often possessed a morphologically abnormal *lin-48p::GFP*+ cell, and lacked a G1 pore autocellular junction (Table 1, Fig. 5). A ventral perspective revealed that the presumptive duct and G1 pore cells adopted adjacent ventral positions in the epidermis (Fig. 5B,C). Thus *lag* mutants resembled *let-60/Ras* partial loss-of-function mutants.

Several lines of evidence suggest that the *lag* duct and G1 pore stacking defects are a secondary consequence of canal cell absence. First, canal cell ablation in wild-type embryos could phenocopy *lag* mutants. Second, a functional LIN-12::GFP reporter (*arIs41*) was not detectably expressed in the duct or G1 pore progenitors during ventral enclosure (Fig. 3E), nor was a LIN-12- and GLP-1-responsive reporter, *ref-1p*::GFP (data not shown); thus Notch signaling is unlikely to impact directly on duct and G1 pore fate specification or tubulogenesis. Third, *lin-12* hypermorphic mutants, which have a single canal cell, had normal duct and G1 pore morphology (Table 1, Fig. 5M). Finally, examination of *lin-12* null mutants or *lag-2*(*q420*) hypomorphic mutants, in which absence of the canal cell is variable, revealed a strong correlation between absence of the canal cell and failure of the duct and G1 pore to stack and undergo tubulogenesis (Fig. 5D-E,G-H,M).

Together, the ablation and Notch mutant data support a model in which the canal cell facilitates duct and G1 pore stacking and tubulogenesis. The canal cell probably provides physical support to the duct and G1 pore as it adheres to the duct during these processes. Stacking and tubulogenesis appear to be independent of canal-cell-expressed *lin-3/EGF*, as these processes were intact in *lin-3* zygotic null mutants, despite defects in cell fate specification (Fig. 2K-L). Duct fate specification also appears to be partially independent of canal cell-expressed *lin-3*/EGF, stacking and tubulogenesis, as it was only mildly affected by absence of the canal cell (Table 1). Nevertheless, as the canal cell does express *lin-3*/EGF, and partial reduction of *let-60*/Ras can mimic canal cell absence, localized LIN-3/EGF expression by the canal cell may help orient relative duct and G1 pore positions during stacking and bias which cell ultimately adopts the duct fate (see Discussion).

Continued signaling through SOS-1 and Ras is required for duct morphogenesis and differentiation

To test the temporal requirements for Ras signaling, we conducted temperature-shift experiments with a *sos-1* (Ras guanine nucleotide exchange factor) temperature-sensitive allele (Fig. 6). *sos-1*(*cs41*) mutants appear essentially normal at 20°C but arrest with excretory system abnormalities when raised at 25°C (Rocheleau et al., 2002). The *cs41* lesion affects the CDC25-related Ras GEF domain of SOS-1, and importantly, *sos-1*(*cs41ts*) lethality is almost completely suppressed by *let-60*(*n1046gf*) (Rocheleau et al., 2002) or *lin-1*(*e1275lf*) mutations (Fig. 6A), indicating that lethal defects are caused by a failure in Ras-ERK-mediated signaling. As *let-60 ras* is required only in the duct cell (and not in the G1 or G2 pore or canal cell) for proper excretory function and viability (Yochem et al., 1997), we further infer that any excretory abnormalities of *sos-1*(*ts*) animals reflect requirements for Ras-ERK signaling in the developing duct cell.

In *sos-1*(*ts*) upshift experiments, upshifts before the 1.5-fold stage of embryogenesis could recapitulate the *let-60 ras* zygotic null phenotype, in which the two cells stacked properly but failed to undergo auto-fusion or to express the marker *lin-48p*::GFP, suggesting both had adopted G1-pore-like fates (Fig. 6B,C). The earliest maternal upshifts could occasionally generate adjacent cells, as seen in *let-60*(*n2021*) hypomorphs (data not shown). In *sos-1*(*ts*) downshift experiments, most animals were normal for excretory morphology as long as they were moved to permissive temperature by the bean stage of embryogenesis (Fig. 6C). These results are consistent with the model that Ras signaling and cell fate specification occur as the presumptive duct and G1 pore cells approach the canal cell and undergo tubulogenesis.

Unexpectedly, the *sos-1*(*ts*) temperature-sensitive period for lethal excretory defects extended from the bean stage into the L1 larval stage (Fig. 6D), revealing continued requirements for signaling beyond initial cell fate specification. At least 70% of animals upshifted at the 1.5-fold, twofold, threefold or early L1

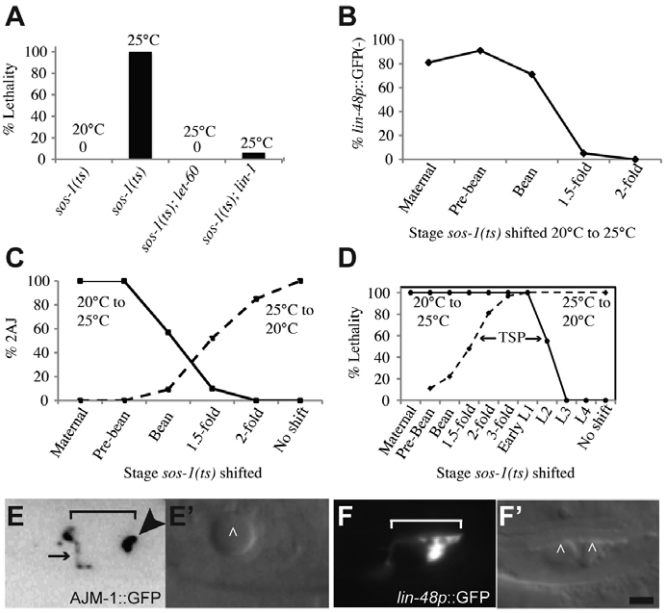

Fig. 6. *sos-1* temperature shift experiments reveal continued requirements during duct morphogenesis and differentiation. (**A**) *sos-1*(*cs41ts*) lethality at 25°C is rescued by *let-60*(*n1046gf*) or *lin-1*(*e1275lf*). *n*>50 for each genotype. (**B**,**C**) *sos-1*(*ts*) animals bearing AJM-1::GFP or *lin-48p*::GFP markers were upshifted or downshifted at the stages indicated. *n*≥20 for each time point. *sos-1* is required before the 1.5-fold stage to promote *lin-48p*::GFP duct marker expression (B) or duct auto-fusion (C). (**D**) The *sos-1*(*ts*) temperature-sensitive period (TSP) for lethality extends from the bean stage of embryogenesis to L2. The majority of animals upshifted before L2 arrested with excretory abnormalities (see C,E,F). Animals upshifted during L2 displayed a scrawny phenotype similar to that reported for *egl-15*/FGFR mutants (DeVore et al., 1995; Roubin et al., 1999). (**E-F'**) Fluid (carats) accumulated in or near the duct in threefold upshifted *sos-1*(*ts*) animals (E',F'), while AJM-1::GFP (E) and *lin-48p*::GFP (F) patterns were unaffected in these same animals. Scale bar: 2 μm.

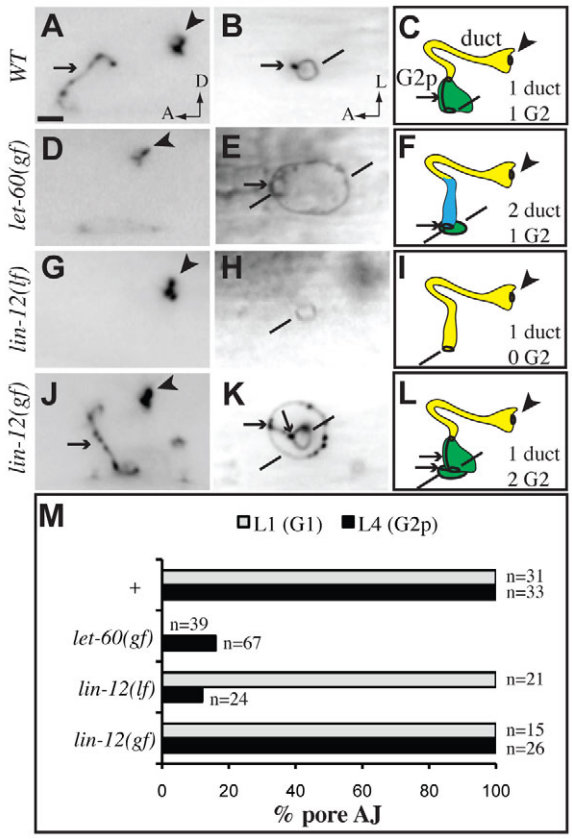

Fig. 7. G1 withdrawal and G2 entry can occur independently. AJM-1::GFP in L4 larvae. (A,D,G,J) lateral views. (B,E,H,K) ventral views. (C,F,I,L) Schematic diagrams. (A-C) In wild type, G2p forms the pore. (**D-F**) In *let-60*(*n1046gf*) mutants, G2p usually wraps around the base of the duct. (**G-I**) In *lin-12*(*n941lf*) mutants, the duct attaches directly to the ventral epidermis after G1 withdrawal. (**J-L**) In *lin-12*(*n137gf*) mutants, the extra G2p cell wraps around the ventral base of the pore. Lines indicate ventral junctions with the epidermis. (**M**) Quantification of junction phenotypes. Scale bar: 2 μm.

stages (*n*>20 each) accumulated fluid either within the excretory tubules or near the canal-duct junction, despite an initially normal junction and *lin-48p*::GFP marker pattern (Fig. 6E,F), suggesting other defects in organ architecture. Although additional studies will be needed to understand the cellular basis of these later defects, we conclude that SOS-1 and Ras, and most likely the entire EGF-Ras-ERK pathway, play additional roles in duct morphogenesis and differentiation.

G1 pore withdrawal can still occur in the absence of G2

When the G1 pore withdraws from the excretory system during L1, a neighboring epidermal cell, G2, moves in to replace it as the pore (Sulston et al., 1983; Stone et al., 2009) (Fig. 1J; Fig. 7A-C,M). By examining Ras and Notch pathway mutants, we were able to address a basic question about the G1-G2 remodeling event: is communication between G1 and G2 important to trigger the withdrawal of G1 and/or the entry of G2 in the excretory system?

As described above, *let-60*(*n1046gf*) mutants invariably lack a G1 pore and have a binucleate duct cell attached directly to the ventral epidermis. In 16% (11/67) of such mutants, G2 still moved in and gave rise to a morphologically normal larval pore cell; in the remainder, G2 (or G2p) wrapped around the base of the duct but did not form a pore of normal height (Fig. 7D-F,M). Thus, G2 entry does not require a 'come here' signal from the G1 pore, but its morphogenesis and ability to insert between the duct and epidermis may be facilitated by the act of G1 withdrawal.

To test the requirements for G2, we used *lin-12*/Notch single mutants, which affect the G2 versus W neuroblast cell fates (Greenwald et al., 1983). *lin-12*(*d*) hypermorphic mutants had two G2 cells, and one of these formed a normal larval pore whereas the other wrapped around its ventral base (Fig. 7J-L,M). Conversely, *lin-12*(*0*) loss-of-function mutants lacked a G2 cell. In such mutants, G1 still withdrew from the excretory system during mid-L1, and the duct then attached directly to the ventral epidermis (Fig. 7G-I,M). Thus, G1 withdrawal does not require a 'go away' signal from G2.

DISCUSSION

We have shown that Notch signaling and Ras signaling function sequentially to control tube development in the *C. elegans* excretory system. Notch signaling is required to generate the canal cell, which is a central organizer of duct and G1 pore

development, serving both as a source of LIN-3/EGF ligand (which contributes to Ras activation) and as a physical attachment site for the duct (which is important for cell stacking and tubulogenesis). Ras signaling influences cell positions, specifies duct versus G1 pore identity, and promotes subsequent aspects of duct morphogenesis and differentiation. Below we propose a model for duct and G1 pore development and discuss similarities and differences between development of the excretory system and development of more complex tube networks.

A biased competition model for excretory duct versus G1 pore fate specification

All excretory tubes are examples of left-right asymmetries in what is a mostly bilaterally symmetric embryo (Sulston et al., 1983; Pohl and Bao, 2010). Notch signaling on the left side of the embryo is required for the earliest of these asymmetries: generation of the excretory canal cell (Lambie and Kimble, 1991; Moskowitz and Rothman, 1996). We propose that Notch-dependent asymmetry of the canal cell leads to the Ras-dependent asymmetry of the excretory duct and G1 pore.

According to this biased competition model, the presumptive duct and G1 pore cells are initially equivalent. As these cells migrate toward the canal cell during ventral enclosure, the left cell has an advantage because of the left-biased asymmetric position of the canal cell; this bias may be strengthened by the presence of cells on the right side with left relatives that undergo cell death. The left cell therefore reaches and adheres to the canal cell first, and also receives earlier or quantitatively more LIN-3/EGF signal. LIN-3/EGF signaling stimulates LET-60/Ras to promote duct identity and strengthen adhesion with the canal cell. Signaling may also trigger production of an unknown lateral inhibitory signal that prevents the presumptive G1 from also responding to LIN-3/EGF. Steric hindrance or differences in relative Ras versus inhibitory signaling levels cause the presumptive G1 to take a more ventral position. Polarization and initial tubulogenesis appear independent of Ras signaling; however, after both cells wrap up into tube shapes, continued LIN-3/EGF signaling from the canal cell (and elsewhere) promotes duct versus G1 pore identity and later aspects of duct morphogenesis and differentiation into a functional tube.

Two aspects of this model can explain the stacking defects of *let-60*/Ras hypomorphs, in which depletion of both maternal and zygotic *let-60/Ras* compromises (but does not eliminate) the earliest steps of signaling. First, the presumptive duct, upon reaching the canal cell, may not adhere to it strongly. Second, the presumptive duct may not express the proposed inhibitory signal in a timely manner. Under conditions in which Ras signaling is reduced but not absent, this would allow the presumptive G1 pore to respond to LIN-3/EGF and compete for a canal-cell-proximal position. Failure of either cell to adhere to the canal cell (as in *lin-12 glp-1*/Notch mutants), or failure to resolve competition between the two cells such that both adhere, could lead to the observed adjacent positions.

Lateral inhibition is a central feature of RTK-mediated branching morphogenesis in several tubular organs (Ghabrial and Krasnow, 2006; Chi et al., 2009) and lateral inhibition of Ras-dependent processes is frequently mediated by Notch signaling (Sundaram, 2005). However, we find no evidence that Notch signaling directly influences excretory duct versus G1 pore cell fates. Differences in cell adhesion and steric hindrance may be sufficient to explain the stacking process, but they are unlikely to explain how only a single duct-like (*lin-48p*::GFP+) cell is specified from the two adjacent precursors in a *lin-12 glp-1*/Notch mutant (Table 1). Therefore, an unknown signaling pathway may be used to mediate lateral inhibition of the duct fate.

Downstream consequences of EGF-Ras-ERK signaling in the excretory duct

In addition to influencing cell positions, EGF-Ras-ERK signaling is both necessary and sufficient for several aspects of duct versus G1 pore identity, including duct-specific patterns of gene expression, auto-fusion and a permanent epithelial identity. This latter difference in duct epithelial permanence versus G1 withdrawal may ultimately explain the lethality of the duct-to-G1 pore fate change in *let-60 ras* null mutants. G1 withdrawal does not depend on cues from the replacement cell G2, but instead appears to be an intrinsically programmed characteristic of the duct and G1 progenitors that is repressed by Ras signaling. Ras may inhibit withdrawal in part by stimulating *aff-1*-dependent auto-fusion to permanently remove the duct autocellular junction and prevent its later unwrapping; however, Ras must have additional effects, as the duct cell still remains permanent in most *aff-1* mutants despite a failure of auto-fusion (Stone et al., 2009).

sos-1(*ts*) temperature-shift experiments suggest that Ras signaling continues to be required after initial fate specification for development of a fully functional duct tube. After its auto-fusion to form a toroid, the duct elongates, changes shape, and elaborates a complex lumen (Stone et al., 2009). The junctions between the duct and its neighboring tubes must be maintained and may undergo further maturation to establish barrier functions and prevent excretory fluid leakage. Finally, the duct-pore junction must be remodeled as G1 withdraws and G2 enters. The continued requirement for *sos-1* as these events are occurring suggests that Ras signaling may directly promote such morphogenetic and differentiation processes.

Most or all of the responses to Ras signaling in the excretory duct appear to be transcriptionally mediated. *sos-1*(*ts*) defects can be rescued by loss of the LIN-1/Ets transcription factor, which is regulated by MPK-1 ERK phosphorylation (Jacobs et al., 1998) and acts as a repressor of the duct fate. *sos-1*(*ts*) defects also can be mimicked by combinatorial loss of LIN-1 and another downstream transcription factor, EOR-1 (a BTB-zinc finger protein) (Howard and Sundaram, 2002; Howell et al., 2010), revealing a second (but redundant) activity of LIN-1/Ets in promoting the duct fate. A challenge for future work will be to connect these transcriptional effectors to downstream targets that control the various cell biological processes of duct auto-fusion, morphogenesis and epithelial maintenance.

Similarities and differences between the excretory system and more complex tube networks

Caenorhabditis elegans excretory tubes are topologically different from epithelial tubes in other renal systems, in that they are each only one cell in diameter. However, similar unicellular tubes have been described in other organ systems, including the *Drosophila* trachea (Ghabrial et al., 2003) and the mammalian microvasculature (Bar et al., 1984). Furthermore, in vitro studies suggest that unicellular tubes may be developmental precursors to some larger bore tubes in the vasculature (Folkman and Haudenschild, 1980; Iruela-Arispe and Davis, 2009).

Despite their topological differences, *C. elegans* excretory tubes and larger multicellular tubes must undergo many similar cell biological processes. For example, initially unpolarized cells must transition to an epithelial state, define an appropriate apical domain, form new junctions, and build a lumen; the difference is that excretory tubes define an intracellular, rather than an extracellular, lumen. Furthermore, distinct tube types must join to form a continuous conduit. The maturing tubes must be structurally strong to withstand internal pressure from their contents, yet flexible enough to elongate and grow as organismal size or physiological demands increase. Finally, some epithelial tube cells, such as the G1 pore, retain the developmental potential to adopt different fates (Jarriault et al., 2008; Mani et al., 2008; Weaver and Krasnow, 2008; Kalluri and Weinberg, 2009; Red-Horse et al., 2010). Given the simplicity of the *C. elegans* excretory system and its amenability to genetic manipulations, further studies in this system should give insights into basic cellular mechanisms involved in these common steps of tubular organ development.

Acknowledgements
We thank Matthew Buechner, Helen Chamberlin, Iva Greenwald, Min Han, Jeff Hardin, Jun Liu, Jim Priess, David Raizen, Paul Sternberg and the Caenorhabditis Genetics Center (University of Minnesota, USA) for providing strains; Craig Stone and Helin Shiah for generating reporters; and Iva Greenwald and John Yochem for helpful discussion and comments on the manuscript. TEM of embryo morphogenesis was originally carried out in collaboration with Ed Hedgecock. This work was funded by NIH GM58540 to M.S. I.A. and V.M. were supported in part by T32 GM008216. J.I.M. was partially supported by the NIH (GM083145), by the Penn Genome Frontiers Institute and by a grant with the Pennsylvania Department of Health, which disclaims responsibility for any analyses, interpretations or conclusions. Deposited in PMC for release after 12 months.

Competing interests statement
The authors declare no competing financial interests.

Supplementary material
Supplementary material for this article is available at
http://dev.biologists.org/lookup/suppl/doi:10.1242/dev.068148/-/DC1

References

Bao, Z., Murray, J. I., Boyle, T., Ooi, S. L., Sandel, M. J. and Waterston, R. H. (2006). Automated cell lineage tracing in Caenorhabditis elegans. *Proc. Natl. Acad. Sci. USA* **103**, 2707-2712.
Bar, T., Guldner, F. H. and Wolff, J. R. (1984). 'Seamless' endothelial cells of blood capillaries. *Cell Tissue Res.* **235**, 99-106.
Beitel, G. J., Tuck, S., Greenwald, I. and Horvitz, H. R. (1995). The *Caenorhabditis elegans* gene *lin-1* encodes an ETS-domain protein and defines a branch of the vulval induction pathway. *Genes Dev.* **9**, 3149-3162.
Berry, K. L., Bulow, H. E., Hall, D. H. and Hobert, O. (2003). A *C. elegans* CLIC-like protein required for intracellular tube formation and maintenance. *Science* **302**, 2134-2137.
Bossinger, O., Klebes, A., Segbert, C., Theres, C. and Knust, E. (2001). Zonula adherens formation in *Caenorhabditis elegans* requires dlg-1, the homologue of the *Drosophila* gene discs large. *Dev. Biol.* **230**, 29-42.
Boyle, T. J., Bao, Z., Murray, J. I., Araya, C. L. and Waterston, R. H. (2006). AceTree: a tool for visual analysis of *Caenorhabditis elegans* embryogenesis. *BMC Bioinformatics* **7**, 275.
Brenner, S. (1974). The genetics of *Caenorhabditis elegans*. *Genetics* **77**, 71-94.
Buechner, M. (2002). Tubes and the single *C. elegans* excretory cell. *Trends Cell Biol.* **12**, 479-484.
Chi, X., Michos, O., Shakya, R., Riccio, P., Enomoto, H., Licht, J. D., Asai, N., Takahashi, M., Ohgami, N., Kato, M. et al. (2009). Ret-dependent cell rearrangements in the Wolffian duct epithelium initiate ureteric bud morphogenesis. *Dev. Cell* **17**, 199-209.
Church, D., Guan, K. L. and Lambie, E. J. (1995). Three genes of the MAP kinase cascade, *mek-2, mpk-1/sur-1* and *let-60 ras*, are required for meiotic cell cycle progression in *Caenorhabditis elegans*. *Development* **121**, 2525-2535.
DeVore, D. L., Horvitz, H. R. and Stern, M. J. (1995). An FGF receptor signaling pathway is required for the normal cell migrations of the sex myoblasts in *C. elegans* hermaphrodites. *Cell* **83**, 611-620.
Dressler, G. R. (2009). Advances in early kidney specification, development and patterning. *Development* **136**, 3863-3874.
Duerr, J. S., Frisby, D. L., Gaskin, J., Duke, A., Asermely, K., Huddleston, D., Eiden, L. E. and Rand, J. B. (1999). The *cat-1* gene of *Caenorhabditis elegans* encodes a vesicular monoamine transporter required for specific monoamine-dependent behaviors. *J. Neurosci.* **19**, 72-84.
Ferguson, E. L. and Horvitz, H. R. (1985). Identification and characterization of 22 genes that affect the vulval cell lineages of the nematode *Caenorhabditis elegans*. *Genetics* **110**, 17-72.
Fire, A., Kondo, K. and Waterston, R. (1990). Vectors for low copy transformation of C. elegans. *Nucleic Acids Res.* **18**, 4269-4270.
Folkman, J. and Haudenschild, C. (1980). Angiogenesis by capillary endothelial cells in culture. *Trans. Ophthalmol. Soc. UK* **100**, 346-353.
Gerhardt, H. (2008). VEGF and endothelial guidance in angiogenic sprouting. *Organogenesis* **4**, 241-246.
Ghabrial, A. S. and Krasnow, M. A. (2006). Social interactions among epithelial cells during tracheal branching morphogenesis. *Nature* **441**, 746-749.
Ghabrial, A., Luschnig, S., Metzstein, M. M. and Krasnow, M. A. (2003). Branching morphogenesis of the *Drosophila* tracheal system. *Annu. Rev. Cell Dev. Biol.* **19**, 623-647.
Greenwald, I. S., Sternberg, P. W. and Horvitz, H. R. (1983). The *lin-12* locus specifies cell fates in *Caenorhabditis elegans*. *Cell* **34**, 435-444.
Hill, R. J. and Sternberg, P. W. (1992). The gene *lin-3* encodes an inductive signal for vulval development in *C. elegans*. *Nature* **358**, 470-476.
Hogan, B. L. and Kolodziej, P. A. (2002). Organogenesis: molecular mechanisms of tubulogenesis. *Nat. Rev. Genet.* **3**, 513-523.
Howard, R. M. and Sundaram, M. V. (2002). *C. elegans* EOR-1/PLZF and EOR-2 positively regulate Ras and Wnt signaling and function redundantly with LIN-25 and the SUR-2 mediator complex. *Genes Dev.* **16**, 1815-1827.
Howell, K., Arur, S., Schedl, T. and Sundaram, M. V. (2010). EOR-2 is an obligate binding partner of the BTB-zinc finger protein EOR-1 in *Caenorhabditis elegans*. *Genetics* **184**, 899-913.
Hwang, B. J. and Sternberg, P. W. (2004). A cell-specific enhancer that specifies lin-3 expression in the *C. elegans* anchor cell for vulval development. *Development* **131**, 143-151.
Iruela-Arispe, M. L. and Davis, G. E. (2009). Cellular and molecular mechanisms of vascular lumen formation. *Dev. Cell* **16**, 222-231.
Jacobs, D., Beitel, G. J., Clark, S. G., Horvitz, H. R. and Kornfeld, K. (1998). Gain-of-function mutations in the *Caenorhabditis elegans* lin-1 ETS gene identify a C-terminal regulatory domain phosphorylated by ERK MAP kinase. *Genetics* **149**, 1809-1822.
Jarriault, S., Schwab, Y. and Greenwald, I. (2008). A *Caenorhabditis elegans* model for epithelial-neuronal transdifferentiation. *Proc. Natl. Acad. Sci. USA* **105**, 3790-3795.
Jiang, Y., Horner, V. and Liu, J. (2005). The HMX homeodomain protein MLS-2 regulates cleavage orientation, cell proliferation and cell fate specification in the *C. elegans* postembryonic mesoderm. *Development* **132**, 4119-4130.
Johnson, A. D., Fitzsimmons, D., Hagman, J. and Chamberlin, H. M. (2001). EGL-38 Pax regulates the ovo-related gene lin-48 during *Caenorhabditis elegans* organ development. *Development*. **128**, 2857-2865.
Kalluri, R. and Neilson, E. G. (2003). Epithelial-mesenchymal transition and its implications for fibrosis. *J. Clin. Invest.* **112**, 1776-1784.
Kalluri, R. and Weinberg, R. A. (2009). The basics of epithelial-mesenchymal transition. *J. Clin. Invest.* **119**, 1420-1428.
Koh, K. and Rothman, J. H. (2001). ELT-5 and ELT-6 are required continuously to regulate epidermal seam cell differentiation and cell fusion in *C. elegans*. *Development* **128**, 2867-2880.
Koppen, M., Simske, J. S., Sims, P. A., Firestein, B. L., Hall, D. H., Radice, A. D., Rongo, C. and Hardin, J. D. (2001). Cooperative regulation of AJM-1 controls junctional integrity in *Caenorhabditis elegans* epithelia. *Nat. Cell Biol.* **3**, 983-991.
Lambie, E. J. and Kimble, J. (1991). Two homologous regulatory genes, *lin-12* and *glp-1*, have overlapping functions. *Development* **112**, 231-240.
Levitan, D. and Greenwald, I. (1998). LIN-12 protein expression and localization during vulval development in *C. elegans*. *Development* **125**, 3101-3109.
Lubarsky, B. and Krasnow, M. A. (2003). Tube morphogenesis: making and shaping biological tubes. *Cell* **112**, 19-28.
Mani, S. A., Guo, W., Liao, M. J., Eaton, E. N., Ayyanan, A., Zhou, A. Y., Brooks, M., Reinhard, F., Zhang, C. C., Shipitsin, M. et al. (2008). The epithelial-mesenchymal transition generates cells with properties of stem cells. *Cell* **133**, 704-715.
Moskowitz, I. P. and Rothman, J. H. (1996). *lin-12* and *glp-1* are required zygotically for early embryonic cellular interactions and are regulated by maternal GLP-1 signaling in *Caenorhabditis elegans*. *Development* **122**, 4105-4117.
Murray, J. I., Bao, Z., Boyle, T. J. and Waterston, R. H. (2006). The lineaging of fluorescently-labeled *Caenorhabditis elegans* embryos with StarryNite and AceTree. *Nat. Protoc.* **1**, 1468-1476.
Nelson, F. K. and Riddle, D. L. (1984). Functional study of the *C. elegans* secretory-excretory system using laser microsurgery. *J. Exp. Zool.* **231**, 45-56.
Nelson, F. K., Albert, P. S. and Riddle, D. L. (1983). Fine structure of the *C. elegans* secretory-excretory system. *J. Ultrastruct. Res.* **82**, 156-171.

Neves, A. and Priess, J. R. (2005). The REF-1 family of bHLH transcription factors pattern *C. elegans* embryos through Notch-dependent and Notch-independent pathways. *Dev. Cell*. **8**, 867-879.
Oka, T., Yamamoto, R. and Futai, M. (1997). Three vha genes encode proteolipids of *Caenorhabditis elegans* vacuolar-type ATPase. Gene structures and preferential expression in an H-shaped excretory cell and rectal cells. *J. Biol. Chem*. **272**, 24387-24392.
Pohl, C. and Bao, Z. (2010). Chiral forces organize left-right patterning in *C. elegans* by uncoupling midline and anteroposterior axis. *Dev. Cell* **19**, 402-412.
Red-Horse, K., Ueno, H., Weissman, I. L. and Krasnow, M. A. (2010). Coronary arteries form by developmental reprogramming of venous cells. *Nature* **464**, 549-553.
Riddle, D. L., Blumenthal, T., Meyer, B. J. and Priess, J. R. (1997). *C. elegans II Monograph Series*, Vol. 33. Plainview, NY: Cold Spring Harbor Laboratory Press.
Rocheleau, C. E., Howard, R. M., Goldman, A. P., Volk, M. L., Girard, L. J. and Sundaram, M. V. (2002). A lin-45 raf enhancer screen identifies eor-1, eor-2 and unusual alleles of Ras pathway genes in *Caenorhabditis elegans*. *Genetics*. **161**, 121-131.
Roubin, R., Naert, K., Popovici, C., Vatcher, G., Coulier, F., Thierry-Mieg, J., Pontarotti, P., Birnbaum, D., Baillie, D. and Thierry-Mieg, D. (1999). let-756, a *C. elegans* fgf essential for worm development. *Oncogene* **18**, 6741-6747.
Santella, A., Du, Z., Nowotschin, S., Hadjantonakis, A.-K. and Bao, Z. (2010). A hybrid blob-slice model for accurate and efficient detection of fluorescence labeled nuclei in 3D. *BMC Bioinformatics* **11**, 580.
Sapir, A., Choi, J., Leikina, E., Avinoam, O., Valansi, C., Chernomordik, L. V., Newman, A. P. and Podbilewicz, B. (2007). AFF-1, a FOS-1-regulated fusogen, mediates fusion of the anchor cell in *C. elegans*. *Dev. Cell* **12**, 683-698.
Segbert, C., Johnson, K., Theres, C., van Furden, D. and Bossinger, O. (2004). Molecular and functional analysis of apical junction formation in the gut epithelium of *Caenorhabditis elegans*. *Dev. Biol*. **266**, 17-26.
Shakya, R., Watanabe, T. and Costantini, F. (2005). The role of GDNF/Ret signaling in ureteric bud cell fate and branching morphogenesis. *Dev. Cell* **8**, 65-74.
Simske, J. S., Kaech, S. M., Harp, S. A. and Kim, S. K. (1996). LET-23 receptor localization by the cell junction protein LIN-7 during *C. elegans* vulval induction. *Cell* **85**, 195-204.
Singh, N. and Han, M. (1995). *sur-2*, a novel gene, functions late in the *let-60 ras*-mediated signaling pathway during *Caenorhabditis elegans* vulval induction. *Genes Dev*. **9**, 2251-2265.
Stone, C. E., Hall, D. H. and Sundaram, M. V. (2009). Lipocalin signaling controls unicellular tube development in the *Caenorhabditis elegans* excretory system. *Dev. Biol*. **329**, 201-211.
Struhl, G., Fitzgerald, K. and Greenwald, I. (1993). Intrinsic activity of the Lin-12 and Notch intracellular domains in vivo. *Cell* **74**, 331-345.
Sulston, J. E. and Horvitz, H. R. (1977). Post-embryonic cell lineages of the nematode *Caenorhabditis elegans*. *Dev. Biol*. **56**, 110-156.
Sulston, J. E., Scheirenberg, E., White, J. G. and Thomson, J. N. (1983). The embryonic cell lineage of the nematode *Caenorhabditis elegans*. *Dev. Biol*. **100**, 64-119.
Sundaram, M. V. (2005). The love-hate relationship between Ras and Notch. *Genes Dev*. **19**, 1825-1839.
Sundaram, M. V. (2006). RTK/Ras/MAPK signaling (February 11, 2006). In *WormBook* (ed. The *C. elegans* Research Community, WormBook), doi/10.1895/wormbook.1.80.1, http://www.wormbook.org.
Tiensuu, T., Larsen, M. K., Vernerrson, E. and Tuck, S. (2005). *lin-1* has both positive and negative functions in specifying multiple cell fates induced by Ras/MAPK signaling in *C. elegans*. *Dev. Biol*. **286**, 338-351.
Totong, R., Achilleos, A. and Nance, J. (2007). PAR-6 is required for junction formation but not apicobasal polarization in *C. elegans* embryonic epithelial cells. *Development* **134**, 1259-1268.
Tuck, S. and Greenwald, I. (1995). *lin-25*, a gene required for vulval induction in *Caenorhabditis elegans*. *Genes Dev*. **9**, 341-357.
Weaver, M. and Krasnow, M. A. (2008). Dual origin of tissue-specific progenitor cells in *Drosophila* tracheal remodeling. *Science* **321**, 1496-1499.
Yochem, J., Sundaram, M. and Han, M. (1997). Ras is required for a limited number of cell fates and not for general proliferation in *Caenorhabditis elegans*. *Mol. Cell. Biol*. **17**, 2716-2722.
Yoshimura, S., Murray, J. I., Lu, Y., Waterston, R. H. and Shaham, S. (2008). *mls-2* and *vab-3* control glia development, *hlh-17*/Olig expression and glia-dependent neurite extension in *C. elegans*. *Development* **135**, 2263-2275.
Zeisberg, E. M., Tarnavski, O., Zeisberg, M., Dorfman, A. L., McMullen, J. R., Gustafsson, E., Chandraker, A., Yuan, X., Pu, W. T., Roberts, A. B. et al. (2007). Endothelial-to-mesenchymal transition contributes to cardiac fibrosis. *Nat. Med*. **13**, 952-961.